*Carbohydrate Research*, 176 (1988) 17–29
Elsevier Science Publishers B.V., Amsterdam – Printed in The Netherlands



# ACCESSIBLE CONFORMATIONS OF THE β-D-(2→1)- AND -(2→6)-LINKED D-FRUCTANS INULIN AND LEVAN

ALFRED D. FRENCH
*Southern Regional Research Center, P.O. Box 19687, New Orleans, Louisiana 70179 (U.S.A.)*
(Received April 13th, 1987; accepted for publication in revised form, October 10th, 1987)

## ABSTRACT

Accessible conformations of the linear D-fructofuranans inulin having β-D-(2→1) and levan (phlein, or phlean) β-D-(2→6) linkages were surveyed with the computer program NHMAP. This program rates individual conformations as allowed if a model can meet glycosidic bond-angle and hard-sphere, interatomic-distance criteria. Molecules of D-fructofuranose have two primary alcohol groups that can rotate, changing the positions of the hydroxyl groups on C-1 and C-6. The C-1–O-1 bond is part of the backbone of inulin, and the C-6–O-6 bond is similarly part of levan. Through steric interference, the other such group also affects the possible conformations of the polymer. Including rotations of both primary alcohol groups in conformational analyses requires substantially more computer time than is needed for simpler polysaccharides. Each polymer has three single bonds that link the fructofuranose rings, and rotations about these bonds permit a large variety of molecular shapes. Despite this degree of molecular flexibility, the use of various starting, monomeric-ring geometries further expands the range of allowed polymeric shapes. Models of both polymers can be either right- or left-handed, although more right-handed models of inulin were allowed; most levan models were found to be left-handed. The depiction of allowed shapes for inulin is similar to one previously published for dextran.

## INTRODUCTION

Inulin and levan, unbranched (2→1)- and (2→6)-linked polymers of β-D-fructofuranose, occur widely in the plant kingdom. Although levans generally result from microbial metabolism, similar polymers are produced by higher plants. All such (2→6)-D-fructofuranose polymers, referred to herein as levans, are said to belong to the phlein or phlean group. Members of either the inulin group or the phlein group are properly called D-fructans, not D-fructosans. Inulin, levan, and branched D-fructans may all exist in the same plant, where they serve as storage carbohydrates and are presumed to enhance the properties of cold- and drought-resistance[1].

Inulin is maintained in solution in the living cell, even though it is almost insoluble (<0.5%) in water at room temperature[2]. At 60°, aqueous solutions containing ~47% of inulin can be prepared if the inulin had previously been precipitated with ethanol. Samples crystallized from cooled, aqueous solution dissolved to only the extent[2] of ~1.5% at 60°. These different solubilities probably result from different molecular conformations.

The objective of the present work was to determine the ranges of likely molecular conformations for inulin and levan molecules by using computer modeling. This is the first reported conformational analysis of levan; Marchessault *et al.*[3] had described the structure of inulin that had been crystallized from supersaturated, aqueous solution. Based on studies of the potential energy of the disaccharide (inulobiose), and on electron diffraction, powder X-ray diffraction, and density measurements, they proposed a helical structure having 5-D-fructofuranose residues per repeat of 1080 pm. They were unable to determine whether those helices are left- or right-handed. Marchessault *et al.*[3] also cited the degree of flexibility that results from the three-bond linkage between the furanose rings, and, looking towards work to be done in the future, the importance of the flexibility arising from within the furanose ring.

The present work explores the effects of flexibility within the D-fructofuranose ring, and includes the effects of an extended polymer chain instead of the inulobiose dimer used by Marchessault *et al.*[3] to model inulin. Several different monomeric geometries, a range of glycosidic angles, and a variety of positions of the primary alcohol groups (O-1 and O-6) were used. Previous work on amylose[4] had shown the necessity of a variety of monomeric geometries and glycosidic angles in order to construct stereochemically sound models of the seven major, known allomorphs, and described a technique for quickly modeling polymers and for reporting results when a number of conformational variables are considered.

These improvements have opposing effects on the number of allowed conformations. Consideration of atomic interactions beyond those arising from the disaccharide (*e.g.*, between helix turns) decreases the number of allowed polymeric conformations compared to those deduced from the disaccharide alone. On the other hand, greater flexibility should increase the number of allowed conformations.

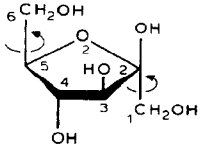


Fig. 1. Atomic numbering for β-D-fructofuranose.

Surveying the possible conformations for inulin and levan requires substantial computational effort, because of the presence of two $-CH_2OH$ groups that can rotate about their bonds to the furanose ring (see Fig. 1). In inulin and in levan, one of the rotating groups participates in the three-bond linkage between monomeric groups. In models of D-fructans, the other primary alcohol group can interfere with helix formation. Therefore, conformational analysis of D-fructans is even more demanding than the study of the $\alpha$- and $\beta$-D-(1→6)-glucans dextran and pustulan. Although the D-glucans also have three-bond linkages, they lack the second rotating group and are composed of (less-flexible) D-glucopyranose rings.

## MODELING AND COMPUTATIONAL DETAILS

The structure of the D-fructofuranose ring and its numbering are shown in Fig. 1. Linkages for inulin and levan are depicted in Figs. 2a and 2b, respectively. Although the endocyclic bonds of the furanose ring are not involved in the backbone of inulin, they are part of the levan backbone.

The NHMAP program[4] requires a set of spatial coordinates for the atoms in the monomeric unit. A convenient source for such coordinates is the crystallographic literature on oligosaccharides containing D-fructofuranose rings. In addition to the coordinates obtained from the neutron-diffraction, single-crystal study of sucrose[5] used earlier[3], sets were taken from X-ray diffraction studies of raffinose[6], planteose[7], and 1-kestose[8]. The molecule of 1-kestose includes two D-fructofuranose rings; both were used.

Table I gives selected torsion angles and virtual bond-lengths for these D-fructose rings. The singly primed residue from 1-kestose has some parameters that differ radically from those of other D-fructofuranose rings. These differences in molecular geometry are so great that the 3- and 4-hydroxyl groups, equatorial in the other residues, are axial in the singly primed residue[8]. The extent of these differences is indicated by the short distance between C-1 and O-4.

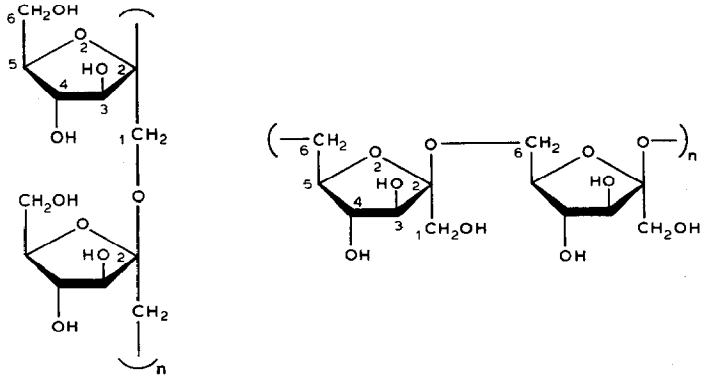

Fig. 2. The inulin (left) and levan (right) linkages.

TABLE I

SELECTED, VIRTUAL BOND-LENGTHS AND TORSION ANGLES FOR D-FRUCTOFURANOSE RINGS

| *Parameter* | *Planteose* | *Raffinose* | *Sucrose* | *Kestose'* | *Kestose''* |
|---|---|---|---|---|---|
| *Virtual bond lengths (pm)* | | | | | |
| C-1–O-2' | 238.3 | 236.3 | 241.8 | 245.5 | 239.8 |
| C-1–O-3 | 322.6 | 325.3 | 331.5 | 373.5 | 323.4 |
| C-1–O-4 | 480.3 | 489.6 | 480.1 | 321.1 | 488.4 |
| C-1–C-6 | 477.3 | 476.4 | 475.9 | 459.0 | 478.1 |
| O-2'–C-6 | 394.0 | 412.2 | 395.4 | 385.1 | 374.2 |
| O-2'–O-3 | 266.9 | 265.2 | 274.4 | 257.0 | 267.9 |
| O-2'–O-4 | 434.1 | 446.5 | 441.5 | 437.7 | 421.2 |
| *Torsion angles* | | | | | |
| C-2–C-3–C-4–C-5 | 38.871 | 38.722 | 35.042 | −29.383 | 40.455 |
| C-3–C-4–C-5–O-2 | −149.592 | −152.311 | −148.413 | −92.564 | −146.611 |
| C-4–C-5–O-2–C-2 | 9.055 | 16.058 | 8.063 | −15.230 | .599 |
| C-5–O-2–C-2–C-3 | 15.916 | 9.644 | 14.655 | −3.683 | 25.053 |
| O-2–C-2–C-3–C-4 | −34.535 | −30.867 | −31.183 | 21.118 | −40.766 |
| C-4–C-5–C-6–O-6 | −179.850 | −173.901 | 49.324 | −178.059 | −177.185 |
| O-2–C-5–C-6–O-6 | 63.499 | 68.883 | −69.554 | 64.556 | 64.748 |
| O-2'–C-2–O-2–C-5 | −100.693 | −110.397 | −102.417 | −120.745 | −88.512 |
| O-2'–C-2–C-3–C-4 | 85.109 | 89.995 | 87.624 | 141.245 | 77.194 |
| O-1–C-1–C-2–O-2 | −65.602 | −59.111 | 171.373 | 179.179 | −57.186 |
| O-1–C-1–C-2–O-2' | 172.471 | −179.302 | 50.614 | 56.498 | 179.219 |

By varying $n$ and $h$ and allowing a range of linkage bond-angles, the NHMAP program implicitly varies the rotational positions of the monomers about the bonds to the oxygen atom in the linkage (the $\phi,\psi$ angles). However, the monomeric coordinates must be modified outside the NHMAP program in order to provide rotation about the abonds to the $-CH_2OH$ groups. For monomers to be used in models of inulin, the C-1–O bonds were stepped through 18 increments of 20° about the C-1–C-2 bond, starting with C-1–O *cis* to C-2–O-2. The C-6–O bonds of monomers for models of levan were given analogous rotations. The original positions of these bonds in their single crystals (see Table I) were also used in models of inulin.

In the study of inulin, the C-6–O-6 bonds (*cf.*, Fig. 2) were initially left in the orientations found in the single crystals. Rotation was not expected to affect the range of allowed conformations strongly, because O-6 is comparatively distant from the C-1 and C-2 atoms that are components of the inulin linkage. In the case of levan, O-1 is adjacent to the C-2–O bond of the linkage, and is free to rotate about the C-1–C-2 bond. The position of O-1 was therefore expected to affect markedly the extent of allowed polymeric conformations. Hence, it was stepped through 20° increments, starting with C-1–O-1 *cis* to C-2–O-2. The original position was also used, for a total of 19 positions. Torsional energies for any of these rotations were not considered. Because of increased computer time required to evaluate fully the effects of rotation of O-1, only the two D-fructose residues from 1-kestose were used.

Although both inulin and levan have a terminal D-glucose residue, the computer models were constructed only from D-fructofuranose residues; the results apply only to the portions of the "real" molecules that are composed of D-fructose. Hydroxyl hydrogen atoms were not considered in the analysis. No accounting for potential hydrogen-bonds was taken, as it was not considered necessary for assessing whether a conformation is accessible.

Results of the NHMAP analyses are displayed on two-dimensional grid plots of $h$ *vs.* $n$, called $n$–$h$ maps. Model helices, which all possess screw symmetry, were tested at increments of $\Delta n = \pm 1$ and $\Delta h = 25$ pm. (Convention assigns positive $n$ values to right-handed helices, and negative $n$ values to left-handed ones.)

NHMAP uses a virtual-bond method to construct the parts of a helical model sufficient to assess its stereochemical feasibility. In this method, the virtual bonds (O-2′–O-1 for inulin; O-2′–O-6 for levan) are first positioned to conform to the $n$–$h$ gridpoint in question. The monomers are then rotated about their virtual bonds in increments of 5°, in an attempt to find a satisfactory, linkage bond-angle. Subsequently, a position is sought that lacks short interatomic distances. Linkage-bond angles (C-2–O–C-1′ for inulin and C-2–O–C-6′ for levan) were accepted when in the range of 110 to 122°. Atomic radii used were $r_C = 150$, $r_O = 130$, and $r_H = 90$ pm. The distance between two atoms was considered short when it was less than the sum of their radii.

## RESULTS

*Inulin.* — The $n$–$h$ map for inulin is shown in Fig. 3. Although the largest $n$ values shown are ±9, helices with values of ±12 or greater were also found during

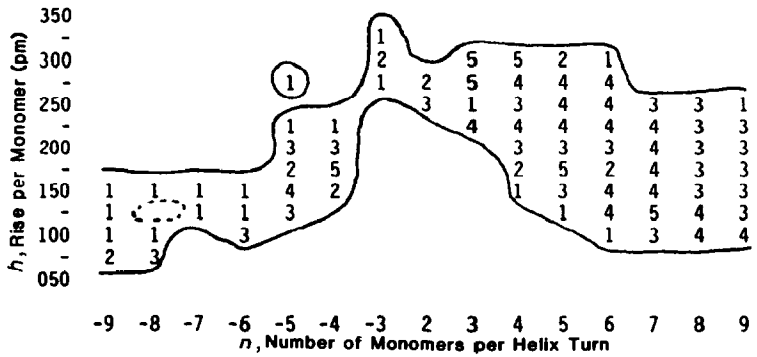


Fig. 3. The $n$–$h$ map for inulin. [The area between the lines represents allowed conformations, except for the area within the dotted line. No allowed models were found at that point. The numbers indicate the number of different monomeric geometries (maximum of 5) that permitted formation of the particular helix.]

limited probes of the extended conformational space. However, such large helices are unlikely in the solid state, because they would pack inefficiently. In solution, such flexible molecules would be likely to be random coils, and segments corresponding to such large helices would seldom occur. The minimal helix pitch $p$ ($p = n \times h$) ranges between 500 and 700 pm.

The left-handed models appear to be relatively inflexible, because allowed models were often produced by only a single monomeric geometry or O-6 position, or both. Only three of the 25 allowed left-handed *n–h* points were allowed by more than one of the 19 positions of O-1 that were tried. Of those 25 *n–h* points, only 11 could be generated by more than one of the five monomeric geometries. The geometry from sucrose permitted only one left-handed model to be formed. Later, analysis showed that his limitation arose from the orientation of its O-6 group in the original *gauche* position. Effects of changes in the O-6 position are discussed later.

On the other hand, all five geometries permitted the formation of helices with $n = +3$ and $+4$ when $h = 300$ pm. All but six of these 49 allowed, right-handed gridpoints (including the two models with $n = 2$) could be generated from more than one of the initial monomeric geometries. Twenty-five allowed gridpoints accommodated more than one O-1 position.

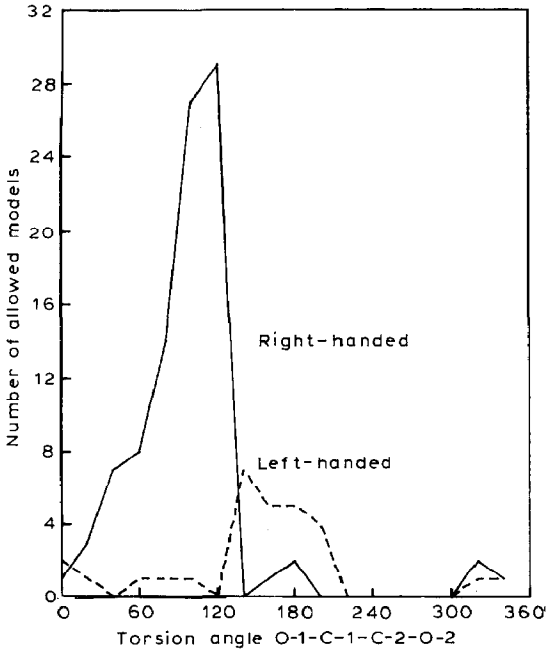


Fig. 4. The effects of changes in the torsion angel O-1–C-1–C-2–O-2 on the number of allowed models of inulin. [The allowed models were built by using the various monomeric geometries, but with O-6 fixed in the initial positions.]

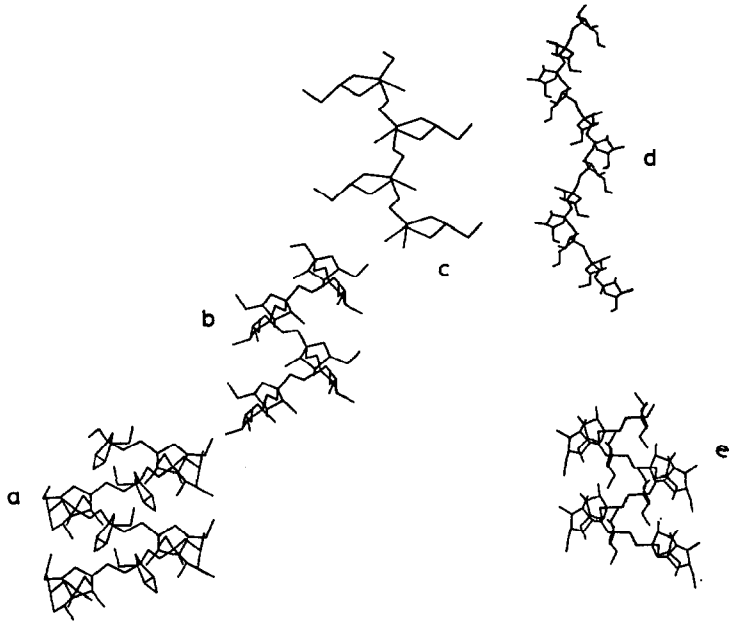


Fig. 5. Sample of allowed models of inulin: a, $n = -6$, $h = 125$ pm; b, $n = 4$, $h = 175$ pm; c, $n = 2$, $h = 275$ pm; d, $n = 6$, $h = 275$ pm; and e, $n = 6$, $h = 125$ pm.

The helices in the center part of the map (with *low* absolute values of $n$ and *high* values of $h$) were typically generated when the torsion angle O-1–C-1–C-2–O-2 was within the range of $-40$ to 100°. Those indicated in the lower right-hand portion of Fig. 3 were formed with torsion angles between 100 to 120°. Those represented by data presented in the lower left-hand portion (*i.e.*, between $n = -9$ and $n = -4$) progressed from 140 to 200°. Fig. 4 shows the numbers of allowed $n$–$h$ gridpoints permitted by the various O-1 positions. Some of the various accessible, helical shapes of inulin are depicted in Fig. 5.

As already mentioned, only one left-handed model could be generated from sucrose. The major differences between the structures of the D-fructofuranose rings of raffinose and sucrose (see Table I) lie in the torsion angles related to the pendant $-CH_2OH$ groups. Because the groups containing O-1 were rotated as part of the analysis, two monomers differ mainly in their O-6 positions during the modeling studies. Therefore, the coordinates of sucrose were modified by stepping the C-6–O-6 bond in 20° increments about the C-5–C-6 bond and were subjected to $n$–$h$ analyses. Fig. 6 is a plot of the number of allowed $n$–$h$ combinations for both left- and right-handed helices against the position of O-6. Although there is a small variation for the right-handed models, the number of left-handed ones is much more dependent on the O-6 position. The 60° position corresponds closely to the original O-6 *gauche* position. The 300° position is similar to the *trans* position found for the other monomers, and is the position to which Marchessault *et al.*[3] rotated

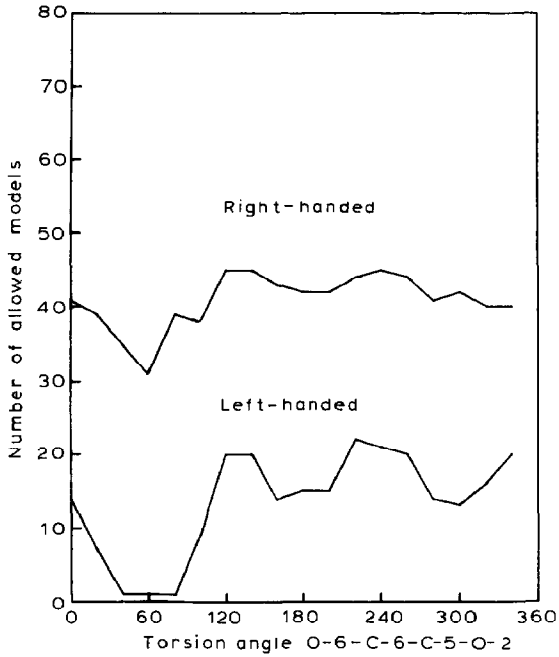


Fig. 6. The effects of changes in the torsion angle O-6–C-6–C-5–O-2 on the number of allowed models of inulin. [The allowed models were built by using only the monomeric geometry from sucrose, but included the incremented variation of the O-1–C-1–C-2–O-2 angle.]

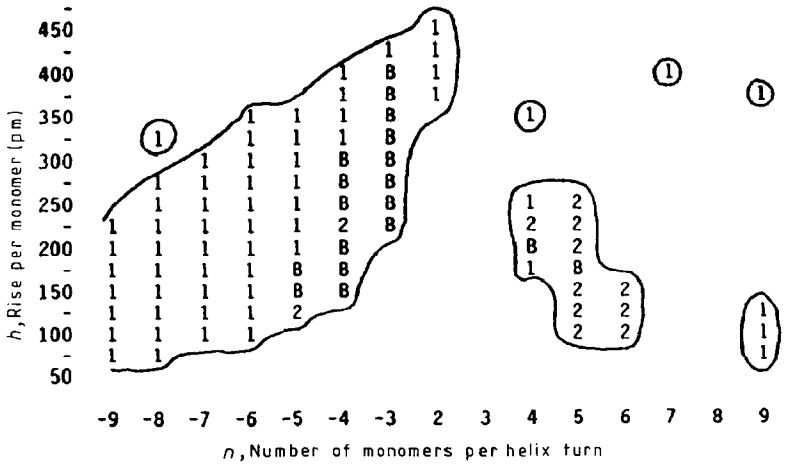


Fig. 7. The *n–h* map for levan. [Allowed models constructed only from the singly primed residue from 1-kestose are designated by "1", those from the doubly primed residue from 1-kestose by 2. Models that could be constructed from both monomers are represented by "B".]

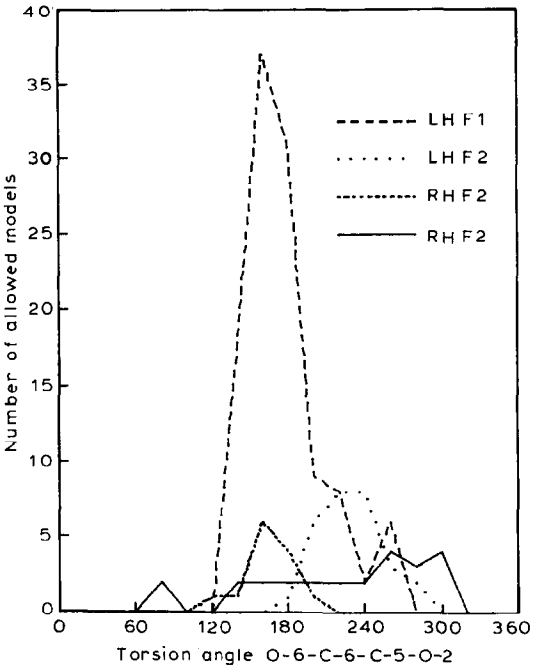


Fig. 8. The effects of changes in the torsion angle O-6–C-5–C-5–O-2 on the number of allowed models of levan. [LH means left-handed, RH means right-handed. The designations F1 and F2 indicate the singly and doubly primed residues from 1-kestose.]

O-6 before performing their analyses. Fig. 6 shows that the *trans* position allows 15 to 20 times as many kinds of helices to form, compared to the *gauche* position, but that some of the "eclipsed" positions (*e.g.*, 240°) allow even more helix types.

The range of allowed, left-handed, *n–h* combinations previously observed (see Fig. 3) was extended by this analysis, filling one gap in the map. New, allowed helices were formed with $h = 225$, $n = -4$, at $h = 175$, $n = (-9 \cdots -6)$, and $h = 125$, $n = 8$. No right-handed *n–h* combinations were found beyond those in Fig. 3.

It is anticipated that were this time-consuming analysis applied to the other monomers, more of the monomers would be able to form more of the *n–h* combinations, especially the left-handed ones, and that the allowed domains would be slightly extended.

*Levan.* — The *n–h* map generated for levan is shown in Fig. 7. Sixty-seven allowed gridpoints were found for left-handed models. Twenty gridpoints represent satisfactory models on the right side, in addition to four gridpoints with $n = 2$. All but two of the left-handed models could be formed by the singly primed residue from 1-kestose. Eighteen of the left-handed models could be formed by the doubly primed, 1-kestose residue. Only the singly primed residue could form helices with $n = 2$. Little overlap in the ability of the two residues to form particular right-handed helices was evident. The separation between zones of allowed, left- and right-handed models indicates that a smooth transition between left- and right-handed molecules would not occur.

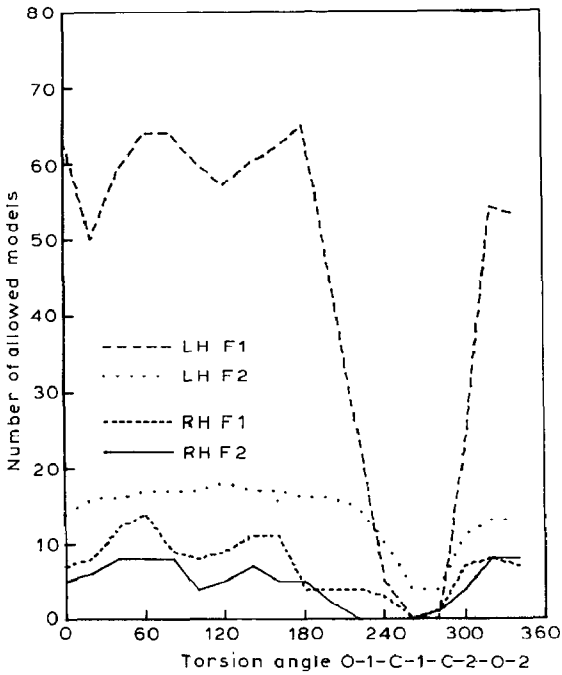


Fig. 9. The effects of changes in the torsion angle O-1–C-1–C-2–O-2 on the number of allowed models of levan. [LH means left-handed, RH means right-handed; F1 and F2 indicate the singly and doubly primed residues from 1-kestose.]

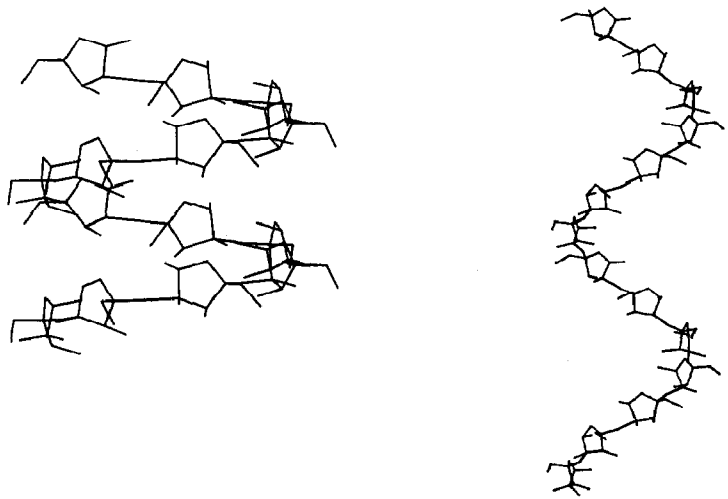

Fig. 10. Levan helices with $n = -7$. [The left helix has an $h$ value of 100 pm; the right helix has $h$ = 300 pm.]

As indicated in Fig. 8, the positions of O-6 giving rise to the most *n–h* grid-points depended on the monomeric geometry and the chirality of the model helices. Allowed helices in the lower left of Fig. 7 could exist when the O-6–C-6–C-5–O-2 torsion angle took values in the range of 140 to 160°. That angle increased as *n* and *h* became increasingly positive and larger, respectively. The positions of O-6 that resulted in formation of allowed helices varied more randomly for the right-handed models. Although a large number of left-handed models was found to be allowed, the aforementioned dependence on monomeric geometry and O-6–C-6–C-5–O-2 angle suggests that such models have little internal, conformational freedom.

Values for the O-1–C-1–C-2–O-2 torsion angle of ~270° effectively prohibit helix formation (see Fig. 9). In this position, the C-1–O-1 bond is *cis* to the C-2–O bond of the linkage. Two of the allowed shapes for levan are shown in Fig. 10.

## DISCUSSION

The main results and conclusions reported by Marchessault *et al.*[3] are generally supported by the results of the present research. Both left-handed and right-handed models with $n = 5$ and $h = 216$ ($p = 5 \times 216 = 1080$) fall in allowed zones. Two other minima, at $n = 3.2$, $h = 3$ ($p = 961$ pm) and at $n = 2.34$ and $h = 214$, are just at the edges of the current *n–h* maps. Only their reported[3] potential minimum, at $n = 4.58$, $h = 4$ pm is disallowed, and they did not describe[3] this minimum as one that might correspond to a helix. Although values of *n* larger than their upper limit of ±8 were found, partly because of the use of a range of glycosidic angles, they are not likely to be important forms. What has been accomplished here, then, is a clarification as to which combinations of *n* and *h* are allowed, and a depiction of the important effects due to monomeric geometry and rotations of the pendant $-CH_2OH$ groups. In particular, the lower boundary of the allowed zone for inulin depicts the effects of spatial confict between helix turns not considered in the previous work. Also, inulin and levan have now been subjected to comparable analyses, so that comparisons are possible.

Because of differences in the solubility of inulin, depending on the type of crystallization employed, the possible occurrence of double helices must be considered. Although this has not been done explicitly in this study, inspection of the *n–h* map indicates that double helices consisting of right-handed strands are possible.

The similarity between the *n–h* map for inulin and one previously published for dextran[9] is remarkable, once compensation is made for the larger range of *h* values for dextran. Dextran, pustulan[9], and inulin appear to be sufficiently flexible to interconvert readily among a large variety of right-handed and left-handed structures. Because each of these polymers is composed of rings linked by three single bonds, it might be concluded that other polysaccharides with three-bond linkages would have similar flexibility. However, the map for levan shows separations

between the sporadically placed, right-handed zones and a zone of left-handed and two-fold helices. The discontinuous character of the *n–h* map for levan suggests that its chirality would not change under normal conditions, probably because a $-CH_2OH$ group is adjacent to the linkage.

This study attempted to define the range of helical structures that are *allowed* under mild conditions. In the separate task of predicting the likely, or *favored* conformations of the polymer, many additional factors must be considered, such as hydrogen bonding and intermolecular interaction. In the case of amylose, however, it was observed that several crystalline conformations lie near the boundaries of the allowed zones of the *n–h* maps, where intramolecular interactions are maximized. The number of monomers that can form helices of a given *n* and *h* is one indication of the entropy, and thus of the likelihood of occurrence of that conformation in solution.

In this work, some uncertainty results from the lack of a wide range of monomeric geometries from the crystallographic literature. (Another ring, from the melezitose monohydrate[10], is nearly identical to the ring from raffinose.) Several of the torsion angles in Table I had ranges of 60°, and such conformational differences had a strong effect on allowed values of *n* and *h*. Some of the smaller ranges in Table I may well expand with further study of the furanose ring. For inulin, new monomeric geometries might increase the allowed values of *h* closer to 370 pm, the greatest likely length of the O-1–O-2′ virtual bond. For levan, more right-handed models might become allowed, as well as extensions of *h* towards the maximum O-2–O-6 virtual-bond length of 510 pm.

Also, the postulate of Natta and Corradini[11] that all monomers in a crystalline solid are identical may not apply in all instances; some overall conformations may be possible that are not regular helices and are thus not predicted by the present method. Better knowledge of the changes in energy associated with rotations of the $-CH_2OH$ groups would help to define parts of the *allowed* areas as *favored*, but the rotomers used herein are considered to be suitable for prediction of *allowed* shapes.

## CONCLUSIONS

Using the *n–h* mapping method, the domains of gridpoints representing allowed, regular helical forms of inulin and levan depended on selection of monomeric geometries, values of the linkage bond-angle, positions of the rotating side-groups, and the choice of atomic radii. The allowed shapes for inulin are similar to those of dextran. The many right-handed models might be characterized as "loose", "robust", or "flexible", because they could be built by using various monomeric geometries and $-CH_2OH$-group orientations. Allowed, left-handed models of inulin were fewer in number, and "tighter". Transition between left- and right-handed helices of inulin appears to be facile.

The allowed models of levan, phlein, or phlean were much more often left-handed. The small number of relatively "tight", right-handed models were isolated

on the *n–h* map, indicating that a change in chirality is not likely. The isolation of the right-handed models appears to arise from conflicts between the linkage atoms and the $-CH_2OH$ group attached to C-2.

ACKNOWLEDGMENTS

Jerry Chatterton suggested this study, and Jesse Bennett provided extensive editorial advice. NHMAP was written by Walt French, and several of the support programs were written by Vincent G. Murphy. Some of the Figures were prepared for publication by Sherman Faught, and Mia Schexnayder assisted with summarizing nearly 1 m of folded, computer printout. Charlie Brooks assisted with several computer-related matters during the consumption of more than one cpu-week's worth of computer time. This work was presented at the New Orleans Carbohydrate Symposium, August 1986.

REFERENCES

1 H. G. PONTIS AND E. DEL CAMPILLO, in P. M. DEY AND R. A. DIXON (Eds.), *Biochemistry of Storage Carbohydrates in Green Plants*, Academic Press, New York, 1985, pp. 205–227.
2 C. F. PHELPS, *Biochem. J.*, 95 (1965) 41–47.
3 R. H. MARCHESSAULT, T. BLEHA, Y. DESLANDES, AND J.-F. REVOL, *Can. J. Chem.*, 58 (1980) 2415–2422.
4 A. D. FRENCH AND W. A. FRENCH, in A. FRENCH AND K. GARDNER (Eds.), *Fiber Diffraction Methods, ACS Symp. Ser.*, 141 (1980) 239–250.
5 G. M. BROWN AND H. A. LEVY, *Acta Crystallogr., Sect. B*, 29 (1973) 790–797.
6 H. M. BERMAN, *Acta Crystallogr., Sect. B*, 26 (1970) 290–299.
7 D. C. ROHRER, *Acta Crystallogr., Sect. B*, 28 (1972) 425–433.
8 G. A. JEFFREY AND Y. J. PARK, *Acta Crystallogr., Sect. B*, 28 (1972) 257–267.
9 A. D. FRENCH, in J. C. ARTHUR (Ed.), *Polymers for Fibers and Elastomers, ACS Symp. Ser.*, 260 (1984) 43–59.
10 D. AVENEL, A. NEUMAN, AND H. GILLIER-PANDRAUD, *Acta Crystallogr., Sect. B*, 32 (1976) 2598–2605.
11 G. NATTA AND P. CORRADINI, *Nuovo Cimento, Suppl.*, 15 (1960) 9.